CONF-820942--29

DE83 009085

Conf-820942--29

Investigation of the Prompt-Neutron Spectrum for Spontaneously-Fissioning ^{252}Cf*

by

W. P. Poenitz
Argonne National Laboratory
Argonne, IL, USA

T. Tamura
Research Participant from Tohoku University
Sendai, Japan

The prompt-fission-neutron spectrum of ^{252}Cf was investigated. The spectrum was measured with Black Neutron Detectors which have a well known efficiency. Considerations of various issues in such measurements lead to an experiment in which a time-calibration pulser, a random pulser, the neutron detector time-of-flight spectrum, the pulse-shape-discriminator gamma time-of-flight spectrum, and the detector-response spectra were simultaneously recorded for the prompt-fission neutrons, transmission through carbon, and shadowbars in a total-cross-section-type measurement. Corrections and associated uncertainties were applied for a large variety of effects which may have been overlooked in many of the previously reported measurements. Preliminary results indicate deviations from a Maxwellian shape toward a Watt-spectrum shape. Agreement is good with the shape differences relative to a Maxwellian from the recent theoretical calculation by Madland and Nix, however, a lower average energy was found.

I. Introduction

The prompt-fission-neutron spectrum of ^{252}Cf is of considerable interest for the interpretation of the fission process as well as for practical applications. It was proposed as a standard for emission spectra measurements (1,2), it is used for detector calibrations (3,4), and it has a direct impact upon the interpretation of $\bar{\nu}$ measurements (5). Substantial experimental effort has been devoted to its determination (see Ref. 6), but the available results are quite often contradictory. Prior to the IAEA-Consultants' Meeting in 1971 (1), two distinctly different groups of values for the average temperature, T, of an assumed Maxwellian spectrum existed (~ 1.41 MeV and 1.58 MeV, respectively). More recent measurements tend to confirm a value of 1.42 MeV, corresponding to an average energy of 2.13 MeV (7-9). However, the post 1971 values are spread over the range from 1.18 to 1.57 MeV (see the summary table in Ref. 6).

Agreement with the Maxwellian-spectrum shape was stressed in the more recent work (7,8), but both neutron excesses and deficiencies at higher or lower energies were noted in the post 1971 measurements (10-12). The apparent satisfaction over finding agreement with a Maxwellian-spectrum shape is in itself surprising: The clear improvement of the basic concept for the derivation of a fission-neutron spectrum shape, that is, taking into account the center-of-mass motion of the fission fragments (Watt-spectrum), suggests that agreement with a Maxwellian-spectrum shape should be viewed with suspicion.

Substantial criticism was directed toward past experimental effort during a recent workshop on fission-neutron spectra (13), more specific critical remarks were expressed in a recent review (6). The unsatisfactory situation is also reflected by the continuing presence of the ^{252}Cf spectrum as a high-priority item on nuclear-data-request lists (14,15). The present measurements were undertaken in order to provide improved data on the ^{252}Cf-fission-neutron spectrum for practical applications as well as for the testing of nuclear model predictions. Consideration of past experiments suggested that there was substantial room for improvements in measurement technique and analysis. A major advantage of the present measurements might well be the use of neutron detectors with well-known efficiencies. However, additional physical, experimental, and instrumental effects which might have been neglected in previous work were investigated and corrected. The results presented here are considered preliminary pending further planned improvements in the measurements and analysis.

II. The Fission Source and Detector

The ^{252}Cf source used in the present measurements was one which was available, but not specifically prepared for this experiment. It consisted of a ^{252}Cf deposit on a 0.0254-cm-thick-platinum disc of 0.953-cm diameter. The source strength was determined by comparison with a ^{252}Cf-reference source. The latter was obtained by vacuum-self-deposition and its absolute fission rate was determined by low-geometry fission-fragment counting. The comparison between the ^{252}Cf source and the reference deposit was made by relative neutron-emission rate measurements using a Marion counter. The source strength was found to be $1.43 \cdot 10^5$ fissions per second at the end of the present measurements.

A gas-scintillation counter was used for the detection of fission events. The counter was described previously (16) but was further modified in order to reduce neutron transmission and scattering corrections. The detector has a cylindrical shape with 16 cm height and a diameter of 22 cm. Neutron entry and exit windows with a radius of 13 cm at the top and bottom of the counter consisted of ~ 0.0036-cm-thick aluminum foil. The ^{252}Cf source was mounted on the inside of one of these windows on the center axis of the detector. A mixture of 85% argon and 15% nitrogen was used as the scintillation gas. Four photo-multipliers were mounted on the outside of the cylindrical surface. The high voltage on each photomultiplier was adjusted to result in approximately the same pulse height spectrum. The lengths of the cables between the anode output of each photo-multiplier and a fast linear mixer were adjusted to result in the same delay for the prompt gamma peak in the time-of-flight spectrum.

The pulse-height spectrum obtained with this fission chamber for the ^{252}Cf-reference source is shown in Fig. 1. The efficiency was determined to be

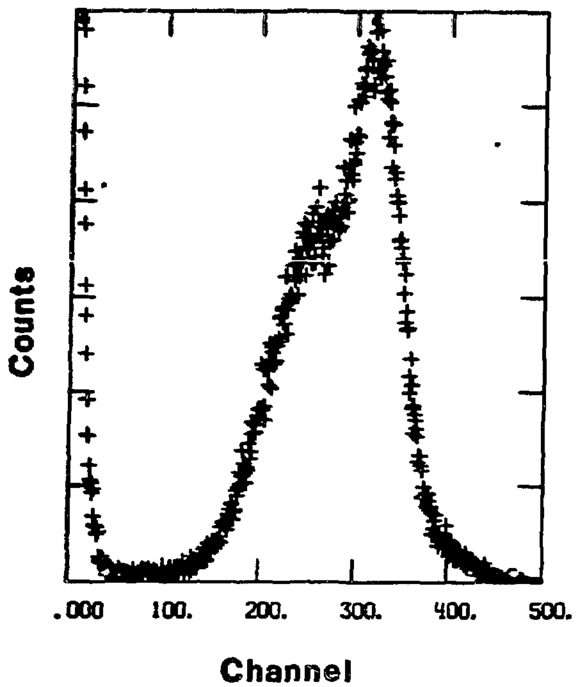

Fig. 1. The Pulse-height Spectrum Obtained with the Gas-scintillation Counter for the ^{252}Cf-Reference Deposit.

≈ 100%. The efficiency for the ^{252}Cf source used in the neutron-spectrum measurements is determined by the losses below the alpha-pile-up and total-fragment absorption. It was determined by measuring the count rate as a function of the fast-discriminator threshold (see Fig. 2), with subsequent extrapolation to zero pulse height. This measurement and the known source strength resulted in the determination of 20 ± 2% losses below the alpha-pile-up and 9 ± 3% total fragment absorption. This shows that substantial fragment energy was lost in the deposit. Fig. 3 shows the fragment-energy spectra obtained for the two deposits perpendicular to the source backings with a surface-barrier detector which supports this conclusion.

The possibility of ^{252}Cf migrated within the chamber was considered and determined at the end of the experiment after removal of the source. It was found as $\lesssim 4 \cdot 10^{-3}$%.

III. The Neutron Detectors and Their Efficiencies

Two Black Neutron Detectors (BND) were used in the present experiments (17,18). The smaller was a cylindrical liquid scintillator with a radius of 7.62 cm and a height of 17.78 cm, and with a cylindrical neutron-entrance channel of 1.9 cm radius and 4.76 cm length. An RCA 8854 multiplier was used for this detector. The larger BND was a cylindrical liquid scintillator with a radius of 10 cm and a height of 37 cm, and with a neutron entrance channel of 1.9 cm radius and 14 cm length. Four 58 DVP photomultipliers were used for this detector. A liquid scintillator medium was formulated for this experiment which had a higher hydrogen content, and appeared to have improved pulse-shape discrimination features relative to NE213.

The efficiency of a BND is ~ 100% based on its design principle, and the deviation from 100% efficiency can be accurately calculated by Monte Carlo techniques. Because this correction and its uncertainty depend mainly on well-known quantities

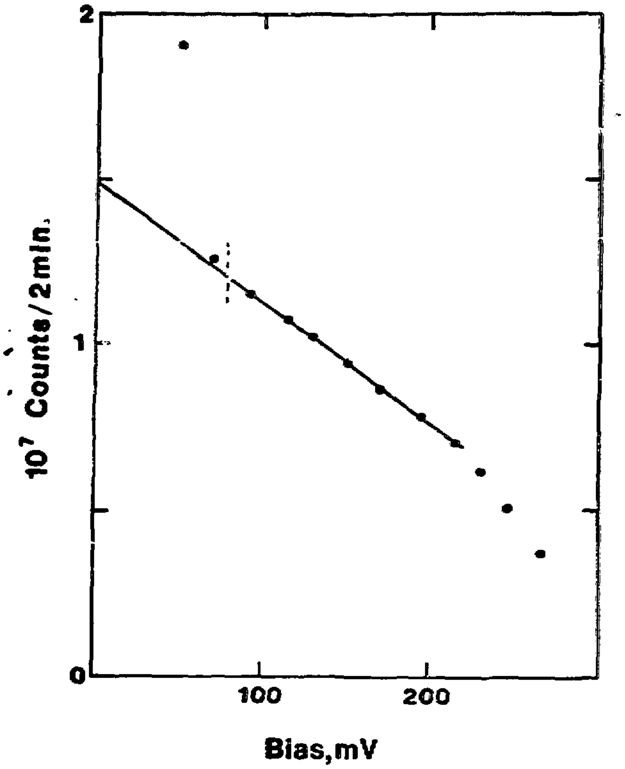

Fig. 2. The Count Rate Obtained with the Gas-scintillation Counter for the ^{252}Cf Source as a Function of the Fast-Trigger Threshold.

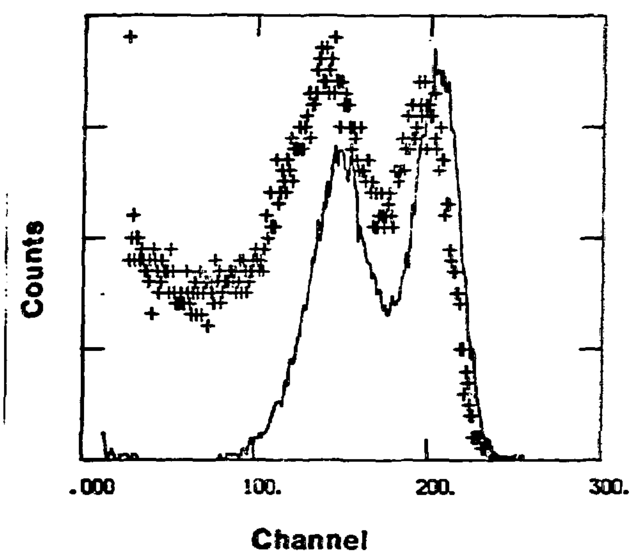

Fig. 3. The Pulse-height Spectra Obtained with a Surface-barrier Detector at 0° for the ^{252}Cf Source and the ^{252}Cf-Reference Deposit.

(transmission through the detector, hydrogen and carbon cross sections, and the detector geometry and composition), this type of detector has a well known efficiency and low uncertainties ($\lesssim$ 1 - 2%). BND's are now used in many laboratories (16-22). Comparisons were made with the associated-partical technique (19,21) and agreement was found within 1.2% and 0.7% at 0.5 - 0.9 MeV and 14.1 MeV, respectively. Indirect support for the $\lesssim$ 1% uncertainty level can be found in recent ^{235}U ($\tilde{n}$,f) cross section measurements (23-25), by comparing results obtained with BND's and with proton-recoil counters or the associated-partical technique.

The smaller detector was used for measurements between ~ 200 keV and 4 MeV where it had an efficiency between 98 and 83%. The larger detector was used between 600 keV and 10 MeV with corresponding efficiencies between 96 and 77%.

IV. The Energy Scale and Resolution

The energy determination and verification is one of the most important factors in ^{252}Cf-spectrum measurements. Energy uncertainties can cause substantially larger spectrum uncertainties than the uncertainties of other quantities. The effects of energy resolution, (which unfortunately is often mistaken for energy uncertainty), can be corrected for, thus reducing the uncertainty of the measured spectrum.

The energy scale in a time-of-flight experiment is based upon three experimentally determined parameters: the time-scaling channel width, Δt, the channel of the center of the prompt-gamma peak, G, and the flight path, ℓ. The energy is determined from

$$E = E_0((1 - \ell^2/c^2T^2)^{-1/2} - 1) \qquad (1)$$

where E_0 is the neutron rest energy, c is the velocity of light and ℓ is the flight path between the source and the front of the detector. Physical processes within the detector will cause an increase of the time at which the neutron will be recorded. The average time given by the center of channel, N, is

$$T + \tau + \tau' = \sum_{N}^{G} \Delta t_i + \frac{\ell}{c} + \frac{H}{c'} \quad . \qquad (2)$$

This assumes that the photomultiplier is at the end of the detector which has a height, H, and a medium, with a light velocity c'. Thus, the additional right-hand terms of Eq. 2 correct for the time the gammas require to be detected. τ is the average time a neutron spends in the detector until the light produced by it exceeds the threshold of the discriminator, and τ' corrects for the time the scintillation light requires to travel the remaining distance to the photomultiplier. The individual relative channel width, Δt_i, can be determined with a random pulser; the average channel width can be determined with a time-calibration pulser. The flight path can be determined within ~ 0.5 - 1.0 mm, and thus contributes little to the energy uncertainties. However, differences in the detection mechanisms for neutrons and gammas might cause larger uncertainties. Because of the sensitivity of the neutron spectrum to energy uncertainties, verification of the energy scale appears mandatory.

The energy resolution is governed by a variety of physical and instrumental effects. These can be grouped into three major components:

a) the time resolution of the electronic components and of the fission chamber, which can be approximated by a Gaussian shape,

b) the time-scaling channel width, which is well defined, and

c) the time-response function of the neutron detector, which is determined by the physical processes within the scintillator.

The component, a, can be obtained from the width of the gamma peak, taking into account that the channel width is already involved. The component, c, can be obtained from Monte Carlo calculations which at the same time yield the average time, τ, the neutron spends in the detector, in order to be detected. Simultaneous verification of the energy scale and the energy resolution can be obtained by measurement of the total neutron cross section of carbon with its well-known resonances.

V. The Experimental Set-up

A schematic of the experimental set-up for the measurement with the smaller BND is shown in Fig. 4. The gas-scintillation counter (GSC) with the ^{252}Cf source (S) was in the cave of a 4π-neutron shield (S-S1 and S-S2) built with lithium-and boron-loaded plastic blocks. A rear-neutron-exit channel

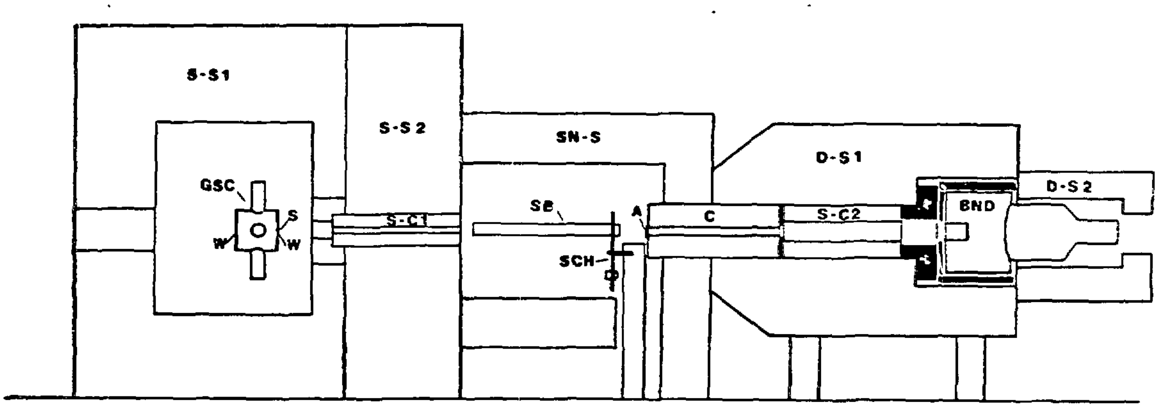

Fig. 4. Schematic of the Experimental Set-up. GSC is the Gas-Scintillation Counter with the ^{252}Cf Source (S) and the Neutron-Entry and Exit Windows. BND is the Black Neutron Detector. SCH is the Eight-Positions-Sample Changer with one of the Three Shadow-bars (SB) and one of the Two Carbon Samples Indicated in the Figure.C is the Main Collimator which Limits the Space Angle of the Source Neutrons for the BND. S-C1 and S-C2 are Shield Collimators. S-S1 (Lithium- and Boron-Loaded Plastic) and S-S2 (Lithium-Loaded Plastic) Form a 4π-Source-Neutron Shield. SN-S is a Neutron Shield for the Neutrons Scattered in the Shadow-bars.D-S1 (A Mixture of Lithiumcarbonate, Water and Lead-pellets) and D-S2 (Lead and Lithium-Loaded Plastic) is a Neutron Detector Shield. A Indicates the Au-Gamma Filter. Black Areas Indicate Lead Shielding.

assured that neutrons scattered within this shield could not reach the neutron detector. Background from neutrons and gammas leaking from the source shield, and scattered within the room, which might still penetrate the detector shield (D-S1 and D-S2), was determined with a shadow-bar (plexiglas). The latter had less than 0.1% neutron transmission. An additional 4π - neutron shield (SN-S) was built around the location of the shadow-bar in order to reduce any possible effect from the neutrons scattered in the shadow-bar or the carbon samples. An eight-position sample changer which moved in a rapid stepping motion was used in order to interchange 3 holes, 3 shadow-bars, and 2 carbon samples for the simultaneous measurement of the fission-neutron spectrum, the carbon transmission, and the shadow-bar background. The first shield collimator (S-C1) was inserted in order to reduce the number of neutrons which impinge on the sample changer, and the number of neutrons which would scatter closer to the neutron detector.

The main collimator, which limits the space angle of the source neutrons detected by the BND, is labeled C in Fig. 4. A second shield collimator (S-C2) reduces the number of neutrons which are scattered in the main collimator and arrive at the neutron detector or near to it. A 0.05-cm-thick gold filter was inserted in front of the main collimator in order to reduce the intensity of the rather soft delayed gammas emitted from the fission fragments. A 0.076-cm-thick-lead filter was placed at the end of the neutron-entrance channel of the BND for the same purpose.

The area between the ^{252}Cf source and the neutron detector was designed to reduce uncertainties in the corrections required for a variety of effects, and to permit an easy Monte Carlo simulation of the spectrum measurements. Neutron inscatter from the main collimator was estimated to be < 0.1%. Neutron inscattering from the first shield collimator was estimated to be $\lesssim$ 0.2%. An additional measurement was made without this shield collimator and without the sample changer.

The detector was located behind the neutron-detector shield (D-S1) and the flight path was extended to ~ 3.50 m for the measurement with the larger BND. The anode signals from the four photomultipliers of the gas-scintillation counter were added in a fast mixer, clipped to ~ 20 nsec, and amplified with a fast-linear amplifier. The stop signal was obtained with a constant-fraction discriminator. The anode signals of the neutron-detector photomultiplier were split and one branch was amplified with a fast-linear amplifier. This signal was used to obtain the neutron-detector-start signal with a constant-fraction discriminator. The second branch was used to obtain a gamma identification signal from a pulse-shape discriminator. A dynode output from the photomultiplier was amplified and an energy signal was obtained from a subsequent linear-gate and stretcher.

The start and stop signals of a time-calibration pulser were added to the start and stop signals from the neutron detector and the fission counter, respectively, with an or-gate. In addition, a random-pulser signal was added to the start signal in the or-gate. The output signals of the or-gates were used to start and stop a time-to-amplitude converter (TAC) using a time range of 1000 nsec. The TAC signals and the pulse-height signals of the neutron detector were converted with amplitude-to-digital converters and recorded with an on-line computer. The origin of the various signals was identified with tag-bits which were obtained from secondary outputs of the respective triggers or the photodiodes on the sample changer. Thus, computer-input words were identified as neutron-detector event, neutron-detector-gamma event, random-pulser event, or time-calibration-pulser event for the fission-neutron spectrum, the carbon transmission, or the shadow-bar background.

end this column here

The simultaneous measurement of these quantities provides a variety of benefits for the interpretation of the experiment. The gamma spectrum can be investigated for structure which might be present (to some extent) as residual background in the neutron spectrum. The shadow-bar-background spectrum indicates the success of the shielding against background from neutron and gamma inscattering from the room. The carbon cross section derived from the measured transmission and the ^{252}Cf spectrum provides a check of the energy scale and of the resolution. The random-pulser spectrum eliminates differential nonlinearity (but, unfortunately it too adds to the statistical uncertainty).

VI. Measurements and Corrections

The results presented here were obtained from three measurement sets. One was obtained with the smaller BND and a flight path of ~ 2.6 m, yielding data in the energy range of 0.2 - 4.0 MeV. A second set was obtained with the larger BND and a flight path of ~ 3.5 m, yielding data in the energy range of 0.7 - 10.0 MeV. The third data set was obtained with the smaller BND, but without the simultaneous measurement of the carbon cross section and without use of the random pulser. Also, the first shield collimator (S-C1 in Fig. 4) was not used in generating this last set. Furthermore, the gold filter was ~ 70% thicker, and a smaller fission chamber was used. Fig. 5 shows the neutron-time-of-flight spectrum obtained with the smaller detector. The

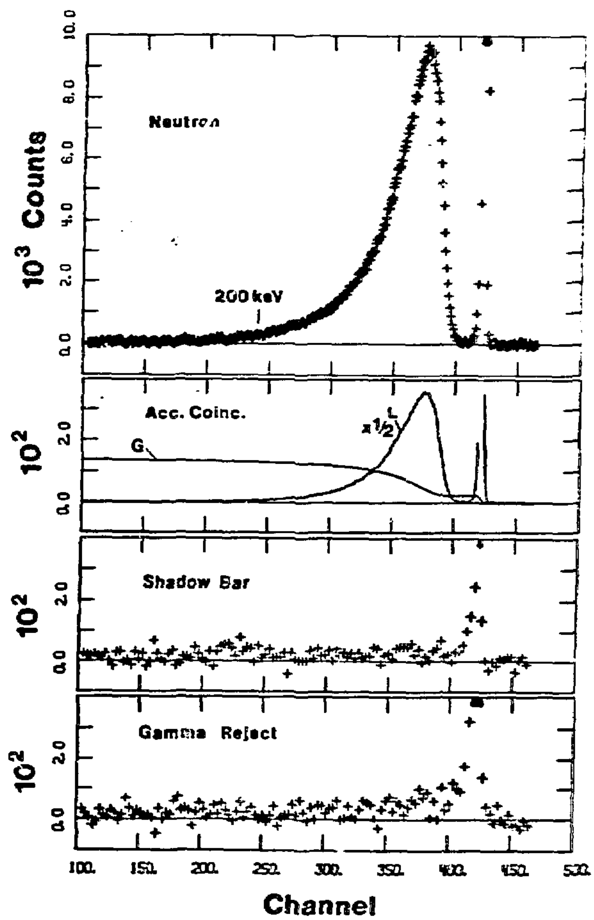

Fig. 5. The Time-of-Flight Spectra obtained with the Smaller Black Neutron Detector and a Flight Path of 2.58 m. Ambient Background has been Subtracted from all Spectra. The Shadowbar Background and the Accidental Coincidence Spectra were Subtracted (Added) from the Neutron Spectrum.

background spectra shown in the same figure were subtracted. Figs. 6 and 7 show the total cross section values obtained with the smaller and the larger BND's respectively. The statistical uncertainties of the cross sections are larger than for the measured spectra not only because of the lower number of counts in the transmission spectra, but also because only two carbon samples were used while there were three positions without samples. The smooth cross section curves in Figs. 6 and 7 were obtained by averaging the calculated transmission through the carbon samples using the ENDF/B-V cross section and a Maxwellian spectrum with the resolution of the present experiment. The carbon total cross section was then derived from this calculated transmission.

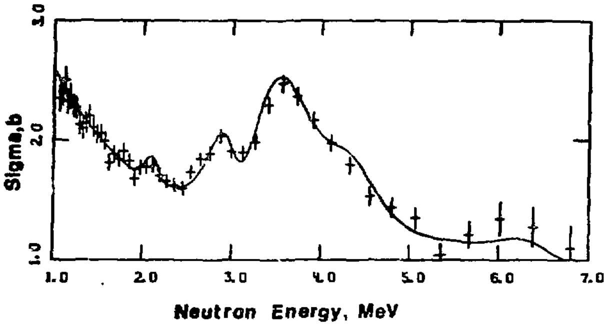

Fig. 6. The Total Cross Section of Carbon Obtained with the Smaller Black Neutron Detector and a Flight Path of 2.58 m. Data were Used only Below 4 MeV.

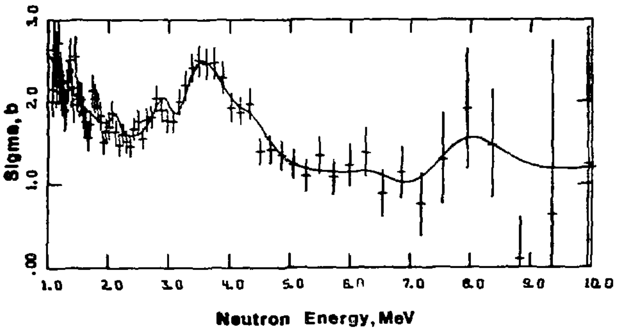

Fig. 7. The Total Cross Section of Carbon Obtained with the Larger Black Neutron Detector and a Flight Path of 3.47 m.

The random-fission-event stop pulses lead to accidental-coincidence losses and gains in the measured time-of-flight spectra. The required corrections were obtained from the associated probabilities:

The accidental-coincidence gains in channel i are given by

$$N_{acc}(i) = \sum_{\ell=i+1}^{\ell max} e^{-N_f t}\left(1 - e^{-N_f \Delta t}\right) N(\ell) \qquad (3)$$

where N_f is the stop rate, and t is the time associated with channel i. Thus, EXP $(-N_f t)$ is the probability that a random stop event does not occur in t, and 1 - EXP $(-N_f \Delta t)$ is the probability that at least one occurs within (the channel width) Δt. Such accidental-coincidence gains ("background") were corrected in some of the previous work (see for example Refs. 10, 26) but a wrong formula was used. The accidental-coincidence gains are, by necessity, the results of accidental-coincidence losses elsewhere in the spectrum. For, the channel, i, associated with the time, t, between the neutron-detector event and the stop pulse, these accidental-coincidence losses are given by

$$N_{acc}(i) = N(i)\left(1 - e^{-N_f t}\right) \qquad . \qquad (4)$$

Both equations neglect a secondary effect which is caused by the dead time of the trigger in the stop branch. This can be shown to be negligible for the present experiment. The accidental-coincidence losses were not corrected in most previously reported ^{252}Cf-spectrum measurements. These corrections were derived independently, however, the problem was previously recognized by Chalupka (27). His formulas are different but they should yield the same result. The formulas for accidental coincidences require the knowledge of the true spectrum, thus, iterative steps were applied. The number of accidental gains is, of course, equal to the number of losses. Losses increase for higher-energy neutrons while the gains are predominant in the low-energy part of the spectrum. (See Fig. 5).

Total-fission-fragment absorption is predominant at angles near 90° relative to the axis perpendicular to the deposit backing. This causes a hardening of the measured spectrum. The required correction can be calculated based upon the kinetics involved. In order to reduce the uncertainty of this correction, measurements of the ratio of the spectra at 0° and near 90° were made. These measurements were made with a flight path of ≈ 1.7 m and the ^{252}Cf deposit mounted in the center of a fission chamber. The corresponding ratio was calculated with the known parameters of the light and heavy fission fragments (26). Best agreement was found for a total-fission-fragment absorption of ~ 7% (see Fig. 8). The required correction (spectrum without absorption versus spectrum with ~ 7% fission-fragment absorption) was ~ 5%.

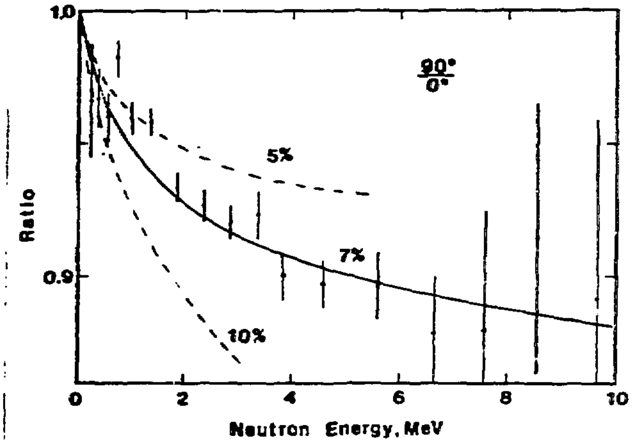

Fig. 8. The Ratio of the Fission-neutron Spectra Observed at ~ 90° and at 0° to the Deposit. The Calculated Curves Indicate Various Amounts of Fission-fragment Absorption at ~ 90°.

Measurements of the spectrum would also be affected, if neutron emision occurs after fragments were already slowed down in the deposit backing. In order to check this, effect, the ratio of the spectra measured at 0° and at 180° to the deposit axis was derived. The result is shown in Fig. 9 and it supports the previous conclusions that neutron emission occurs within 10^{-15} sec. of the fission process (6).

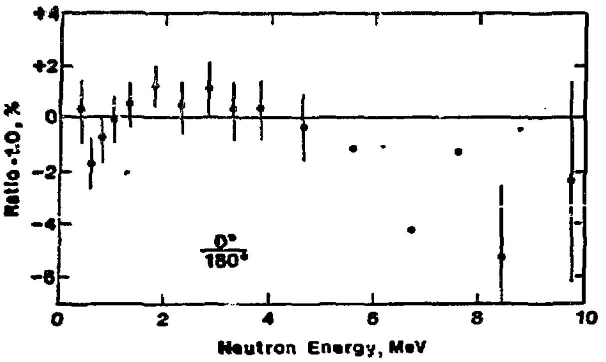

Fig. 9. The Difference from Unity in Percent of the Ratio of the Fission-neutron Spectra Observed at 0° and 180°.

Neutron transmission through the deposit backing, the air of the flight path, the gold filter, and the edges of the collimeter changed the measured spectrum. The corrections were suficiently small and/or the cross sections well enough known to result in insignificant uncertainties for the corrected spectrum. Some of the corrections required for elastic and inelastic scattering events involve energy transfer and result in an experimental spectrum with more low-energy neutrons than the original spectrum. These effects were substantially reduced in the present measurements due to the design of the experiment. Neutrons which scattered in the ≈ 0.05 grams of aluminum forming windows of the GSC and in the ≈ 0.4 grams of the platinum backing could reach the detector. Only the scattering in the platinum backing was significant. The effect due to elastic scattering was corrected by using Legendre-coefficients for elemental platinum (28,29) and taking into account the increase of the interaction probability for neutrons emitted toward 90°. Data on the inelastic scattering in platinum are sparse. Only a few levels (< 1 MeV) were resolved with some cross section data available (29). For inelastic scattering to higher levels an evaporation spectrum was used. Scattering from the two collimators was estimated to be < 0.1% from the collimator in front of the detector and ≲ 0.2% from the collimator in front of the source. Because little energy transfer is involved, these corrections have been deferred but will be included in a Monte-Carlo simulation of the experiment at a later time.

Neutrons which penetrate the detector or which are scattered without being detected might return to the detector after scattering in the photomultiplier or other materials surrounding the neutron detector. The additional neutron-time-of-flight implies a softer measured spectrum. There is an additional advantage in using a BND because this correction is proportional to $1 - \varepsilon_n$, where ε_n is the neutron detector efficiency, which is high for the BND. This correction was < 1% for the present experiment.

Delayed gammas from the fission products are rather soft (30) and were mostly eliminated with the gamma discriminator, and the gamma absorption filters. Support for this was found in consideration of the residual background between the gamma peak and the neutrons in the time-of-flight spectra (see below).

The possibility of neutron production by the alphas emitted in ^{252}Cf decay was considered. The threshold for detecting the fission fragments was set above the alpha-pile-up level, however, some alpha-pile-up trigger pulses cannot be excluded. The (α,n) threhsold in platinum is high enough so that neutron-production should not occur. The possibility of neutron production from other parts of the detector was checked with a strong ^{241}Am alpha source. No effect was found.

The (n, 2n) reaction in platinum contributes some neutrons to the spectrum. The required correction was calculated and found to be negligible (γ,n), (γ,2n) was estimated and also found to be negligible.

After the corrections for accidental coincidences, shadow-bar background and ambient background subtraction were applied, the residual background in the areas between the gamma peak and the neutrons, and below the neutron detection threshold were found to be very small in two of the spectra. The difference for the neutron spectra between not subtracting this residual background or subtracting it by linear interpolation between the two background ranges was ≲ 0.3% at the lowest and higher energies. For the third spectrum this background was somewhat higher. Ultimately, the residual background was subtracted by linear interpolation.

The agreement between all three measured spectra in respective overlap ranges was good.

VII. Results and Discussion

The results from the present measurements were reduced to a lesser number of energies then obtained with the TOF spectra which were identical for the three spectra. The procedure of reducing to this energy grid was described previously (31). A Maxwellian spectrum shape was used for extrapolation to the grid energies. This results in reduced statistical uncertainties and unchanged systematic uncertainties. The three spectra were then normalized to one another in the overlap range and averaged. The final result was normalized to the same number of neutrons in a Maxwellian spectrum with T=1.42 MeV within the range of the present measurements. The difference of the present results from a Maxwellian of T= 1.42 MeV is shown in Fig. 10. The difference of a Watt spectrum from a Maxwellian spectrum of the same average energy (2.13 MeV) is also shown in Fig. 10. The present result deviates from a Maxwellian-spectrum shape toward the Watt-spectrum shape. Madland and Nix (38) recently develped a theoretical approach for calculating fission properties. The ^{252}Cf-fission spectrum obtained from these calculations has an average energy of 2.2791 MeV (38). By using an improved mass formula, a spectrum with a lower average energy of 2.2167 MeV was calculated (39). This spectrum is also shown in Fig. 10 relative to a Maxwellian-Spectra of T = 1.42 MeV.

The average energy of the present result for the ^{252}Cf spectrum was obtained by approximating the low-and-high-energy regions not included in the present measurement with a Maxwellian spectrum of T = 1.42 MeV. The result for the average energy of the present measurement is 2.159 MeV. Fig. 11 shows the present results relative to a Maxwellian spectrum of the same average energy (2.159 MeV). The Watt spectrum is also shown for this average energy. The two spectra calculated by Madland and Nix (38,39) are shown relative to Maxwellian spectra of the respective average energies of 2.2167 MeV and 2.2791 MeV. This shows that the spectra differences relative to Maxwellian spectra of the same average energy are in first order independent of the average energy. Thus, we can conclude that our data support the shape difference between the spectrum calculated by Madland and Nix and a Maxwellian spectrum.

The present data were nevertheless fitted with a Maxwellian sprectrum using the variance-covariance matrix of the data. This led to a temperature of 1.439 MeV which corresponds to the identical average energy as determined from the experimental data.

end this column here

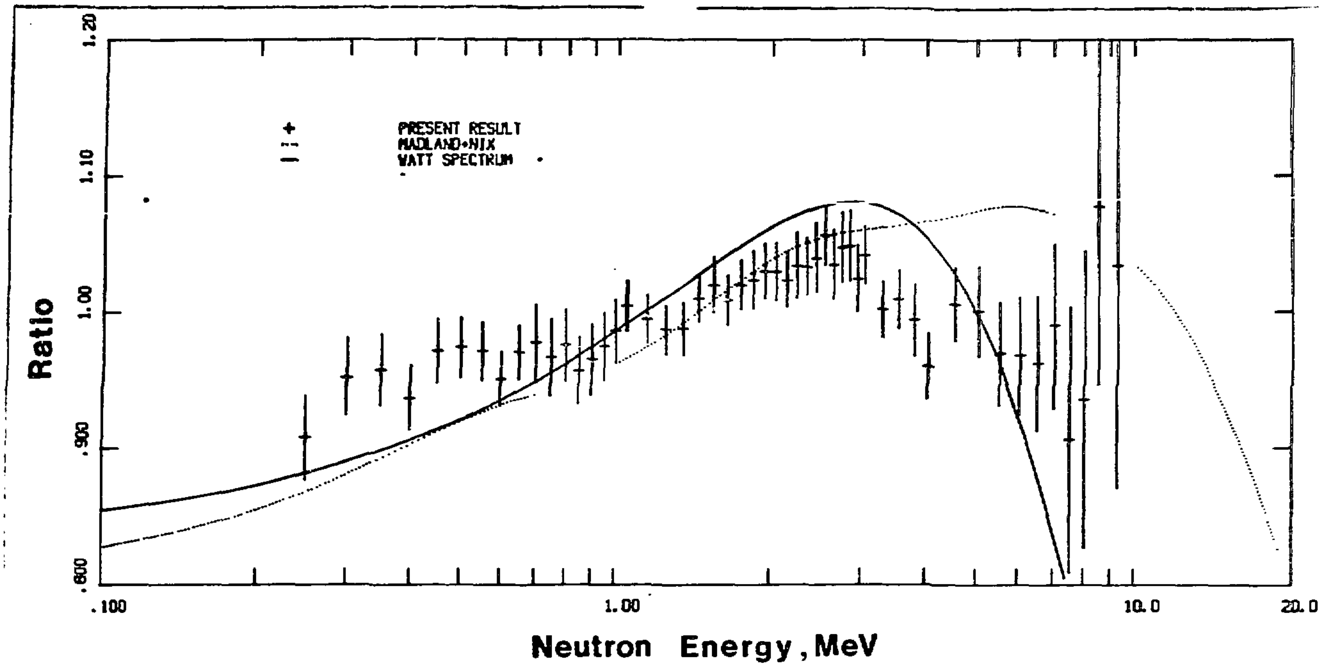

Fig. 10. The Ratio of the Present Results for the ^{252}Cf-Fission-Neutron Spectrum to a Maxwellian with a Temperature of 1.42 MeV ($\bar{E}$ = 2.13 MeV). The Ratios of a Watt Spectrum with the same Average Energy, and of the Theoretical Calculations by Madland and Nix to the Maxwellian are also shown. The Spectrum by Madland and Nix has an Average Energy of 2.2167 MeV.

The present result for the average energy is compared in Table 1 with results from other TOF measurements in the post-1971 area. The present value for the average energy is higher than those obtained in the last three measurements. Complete descriptions of these experiments are not yet available. It is more surprising that the other experiments listed in Table 1 did not result in more substantial differences. This may be due to partial compensation of effects overlooked in these experiments.

The present reuslts are preliminary, pending improvements for some of the corrections and a possible improvement in measurement technique involving a better ^{252}Cf source (and backing) and better statistical accuracy.

Acknowledgements

The present work was supported by the U.S. Department of Energy. Valuable discussions with Drs. A. B. Smith and J. M. Meadows were appreciated. The least-squares fit of the present data and their variance-covariance matrix to a Maxwellian spectrum was carried out by Dr. D. L. Smith.

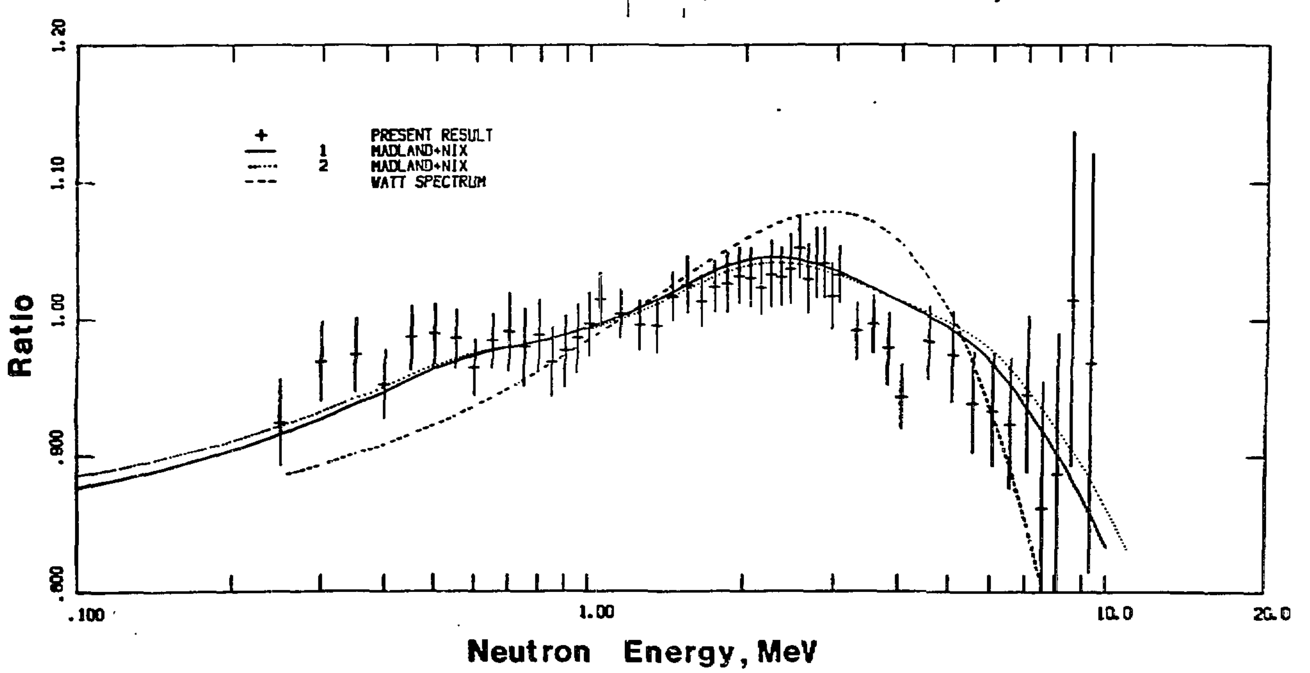

Fig. 11. The Ratio of the Present Experimental Results to a Maxwellian with the same Average Energy (2.159 MeV). The Ratio of the Watt Spectrum is also Shown for the Same Average Energy. The Calculated Spectra by Madland and Nix are Shown Relative to Maxwellian Spectra of the Same Average Energies of 2.2167 MeV and 2.2791 MeV.

end

begin

Table I. Comparison of the Present Result for the Average Energy with other Post 1971 Time-of-Flight Measurements

Reference		Year	$T_{MaxW.}$, MeV	$\bar{E}$, MeV
Green et al.	(10)	1973	1.406 ± 0.015	2.105 ± 0.01
Knitter et al.	(32)	1973	1.42 ± 0.05	2.13 ± 0.08
Kotelnikova et al.	(33)	1976	1.46 ± 0.02	(2.19 ± 0.03)
Batenkov et al.	(34)	1975	1.40	
Blinov et al.	(35)	1977	1.41 ± 0.03	2.12
Nefedov et al.	(36)	1977	1.28	(1.92)
Nefedov et al. (Starostov et at.)	(11)	1978 1981	1.43 ± 0.02	(2.15 ± 0.03)
Bertin		1978	(1.51)	2.27 ± 0.02
Blinov et al.	(7)	1979	1.42	
Bodeman et al.	(8)	1979	1.424 ± 0.013	2.136 ± 0.02
Mon Jiangshen et al.	(9)	1981	1.416 ± 0.023	
Present Result		1982	1.439 ± 0.010	2.159

References

1. Proc. IAEA Consultants' Meeting on Prompt Fission Neutron Spectra, Vienna, 1971.
2. Proc. IAEA Panel on Neutron Standard Reference Data, Vienna, 1974.
3. A. B. Smith et al., NIM 140, 397 (1977).
4. V. A. Vukolov et al., Proc. Conf. Neutr. Physics, Vol. 6, 265, Kiev 1976.
5. J. R. Smith, Summary of a Workshop on Fission Spectra, Los Alamos Report LA-7739-C (ENDF-278), 1978.
6. M. V. Blinov, Proc. IAEA Consultants' Meeting on Neutron Source Properties, Debrecen, p. 79 (1980).
7. M. V. Blinov, Proc. IX Intern., Symp. on the Interactions of Fast Neutrons with Nuclei, Rossendorf (1980).
8. J. W. Boldeman et al., ANS Transactions 32, 733 (1979).
9. Mon Jiangshen et al., Chin. I. of Nucl. Phys. 3, 163 (1981).
10. L. Green et al., NSE 50, 257 (1973).
11. B. I. Starostov et al., INDC (CCP)-1641L (1981).
12. See figures in Ref. 6.
13. Summary of a Workshop on Fission Spectra, Los Alamos Report LA-7739-C (ENDF-278), 1978).
14. Compilation of Requests for Nuclear Data, DOE/NDC-22/U (1981).
15. WRENDA 81/82, World Request List for Nuclear Data, INDC (SEC)-78/URSF (1981).
16. W. P. Poenitz, NSE 53, 370 (1974).
17. W. P. Poenitz, NIM 109, 413 (1973).
18. W. P. Poenitz, Argonne National Laboratory Report, ANL-7915 (1972).
19. G. P. Lamaze et al., NBS Special Publ. 425, Vol. I, 73 (1975), M. M. Meier, NBS Special Publ. 493, 221 (1977).
20. C. Renner, Oak Ridge National Laboratory, private communication (1978).
21. G. Grenier, 3rd. Conf. on Neut. Dos. (1977).
22. Tohoku Univ., Sendai, Japan (1981).
23. W. P. Poenitz, NSE 64, 894 (1977).
24. A. O. Wasson, to be published in NSE (1982).
25. R. Arlt, et al., Tech., Univ. Dresden Reports, 05-43 (1980).
26. H. R. Bowman et al., Phys. Rev. 126, 2120 (1962).
27. A. Chalupka, NIM 165, 103 (1979).
28. A. Langsdorf et al., Argonne National Laboratory, ANL-5567 (1956).
29. A. B. Smith et al., Argonne National Laboratory, ANL-7363 (1967).
30. S. A. E. Johansson, NP 64, 147 (1965).
31. W. P. Poenitz, Proc. Conf. on Nuclear Data Evaluation Methods and Procedures, NEANDC(US)-209, Vol. 1, p. 249 (1980).
32. H. H. Knitter et al., Atomkernenergie 22, 84 (1973).
33. G. V. Kotelnikova et al., INDC (CCP)-81/U (1976).
34. O. I. Batenkov et al., Conf. Neutron Physics, Kiev, Vol. 5, p. 114 (1975).
35. M. V. Blinov et al., NBS Spec. Publ. 493, 194 (1977).
36. V. N. Nefedov et al., Conf. Neutron Physics, Kiev, Vol. 3, p. 205 (1977).
37. A. Bertin et al., CEA-R-4895 (1975).
38. D. G. Madland and J. R. Nix, NSE 81, 213 (1982).
39. D. G. Madland, private communication (1982).

end this column here

end this column here